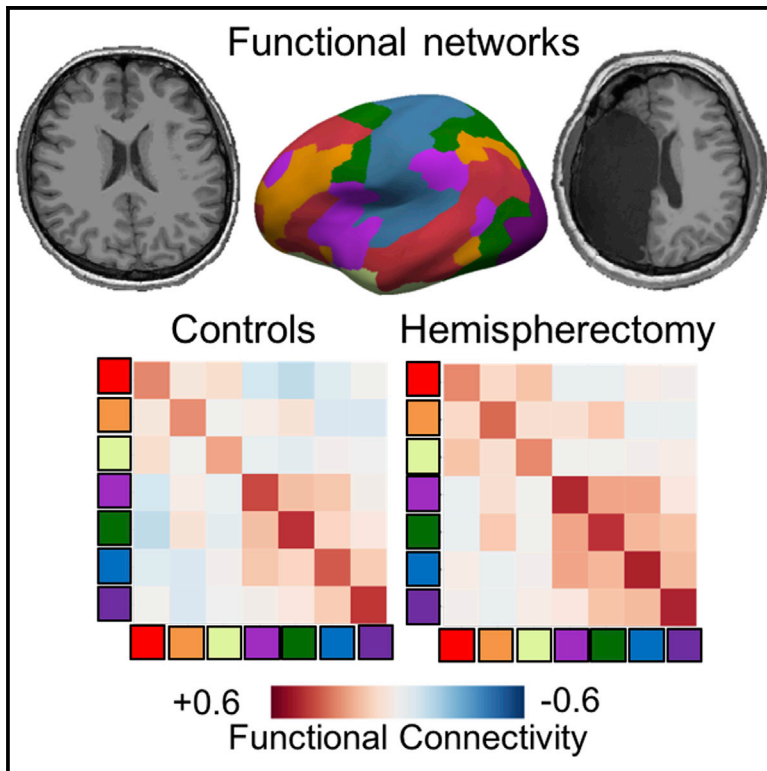**Article**

Intrinsic Functional Connectivity of the Brain in Adults with a Single Cerebral Hemisphere

Graphical Abstract

Authors

Dorit Kliemann, Ralph Adolphs,
J. Michael Tyszka, ..., Remya Nair,
Julien Dubois, Lynn K. Paul

Correspondence

dorit@caltech.edu

In Brief

Kliemann et al. present resting state neuroimaging data in six adults with childhood hemispherectomy, compared to controls. They find an intact functional organization into canonical networks, yet identify an increase in communication between networks—a possible characterization of functional reorganization in hemispherectomy.

Highlights

- Intrahemispheric functional connectivity in 6 adults with childhood hemispherectomy

- Organization of canonical resting-state networks is preserved in intact hemisphere

- Communication between networks is increased compared to controls

- Known functional brain networks support cognition even in highly atypical anatomy

CellPress

Intrinsic Functional Connectivity of the Brain in Adults with a Single Cerebral Hemisphere

Dorit Kliemann,[1,7,*] Ralph Adolphs,[1] J. Michael Tyszka,[1] Bruce Fischl,[2,3,4] B.T. Thomas Yeo,[2,5,6] Remya Nair,[1] Julien Dubois,[1] and Lynn K. Paul[1]

[1]Division of Humanities and Social Sciences, California Institute of Technology, Pasadena, CA 91125, USA
[2]Athinoula A. Martinos Center for Biomedical Imaging, Massachusetts General Hospital, Charlestown, MA 02129, USA
[3]Department of Radiology, Harvard Medical School, Boston, MA 02114, USA
[4]Division of Health Sciences and Technology and Engineering and Computer Science MIT, Cambridge, MA 02139, USA
[5]Department of Electrical and Computer Engineering, Centre for Sleep and Cognition, Clinical Imaging Research Centre, N.1 Institute for Health and Memory
Networks Program, National University of Singapore, Singapore 119077, Singapore
[6]NUS Graduate School for Integrative Sciences and Engineering, National University of Singapore, Singapore 119077, Singapore
[7]Lead Contact
*Correspondence: dorit@caltech.edu
https://doi.org/10.1016/j.celrep.2019.10.067

SUMMARY

A reliable set of functional brain networks is found in healthy people and thought to underlie our cognition, emotion, and behavior. Here, we investigated these networks by quantifying intrinsic functional connectivity in six individuals who had undergone surgical removal of one hemisphere. Hemispherectomy subjects and healthy controls were scanned with identical parameters on the same scanner and compared to a large normative sample (n = 1,482). Surprisingly, hemispherectomy subjects and controls all showed strong and equivalent intrahemispheric connectivity between brain regions typically assigned to the same functional network. Connectivity between parts of different networks, however, was markedly increased for almost all hemispherectomy participants and across all networks. These results support the hypothesis of a shared set of functional networks that underlie cognition and suggest that between-network interactions may characterize functional reorganization in hemispherectomy.

INTRODUCTION

Studying temporal correlations of blood-oxygenation-level-dependent signal (BOLD) as indirect measures of intrinsic functional connectivity with resting-state fMRI has revealed a reliable set of brain networks in healthy people (Biswal et al., 1995; Damoiseaux et al., 2006). A typical set of resting-state networks has now been reproduced in hundreds of studies that are consistent across different anatomical or functional parcellations (Fan et al., 2016; Glasser et al., 2016; Gordon et al., 2016; Yeo et al., 2011). Moreover, these same networks also emerge when differentially activated by different cognitive tasks (Cole et al., 2014; Fox and Raichle, 2007; Smith et al., 2009), reflecting this association in their naming conventions (e.g., default mode network and fron-

toparietal attention network). Studying the connectivity within these networks across large datasets has revealed associations with individual differences in cognition and behavior (Dubois et al., 2018a, Kong et al., 2019) personality (Dubois et al., 2018b), and disease (Castellanos et al., 2013).

This large and rapidly growing literature thus supports the idea of a relatively small set of functional brain networks that underlie all cognition and behavior (Smith et al., 2009), with individual differences reflecting subtle variations in this underlying substrate. However, it is possible to retain remarkably intact cognition despite profoundly atypical neuroanatomy, most notably exemplified in rare cases of hydrocephalus (Feuillet et al., 2007) or large brain lesions (Damasio et al., 1985). Does the compensated level of cognition that can occasionally be found in such patients depend on a different or reorganized set of functional networks, or does mostly intact cognition always go hand in hand with the basic set of resting-state networks? Neither of the above cases (Feuillet et al., 2007; Damasio et al., 1985) has been investigated with resting-state fMRI, and a quantitative answer to this question remains unknown. Here, we tested this question by collecting high-quality resting-state fMRI in a sample of six rare individuals with major anatomical perturbation, high-functioning patients after surgical removal of one cerebral hemisphere (hemispherectomy; Figure 1; Table 1).

Patients who had hemispherectomy in childhood may retain surprisingly high levels of cognitive and sensorimotor abilities (Moosa et al., 2013). Hemispherectomy is a surgical procedure typically used to alleviate certain forms of intractable epilepsy (Jonas et al., 2004) by isolating the affected hemisphere, either by removing it entirely (anatomical hemispherectomy, often including all subcortical structures) or by severing all connections to the functional hemisphere (functional hemispherectomy, with partial anatomic resection) (Kim et al., 2018). There are consequential impairments to sensory and motor functions (described in detail elsewhere, e.g., hemiparesis and hemianopsia; see de Bode and Curtiss, 2000; Moosa et al., 2013), but even these may recover to some extent (Devlin et al., 2003; Liu et al., 2018; Ramantani et al., 2013). Language function has been studied in some detail, also showing near-complete recovery in many
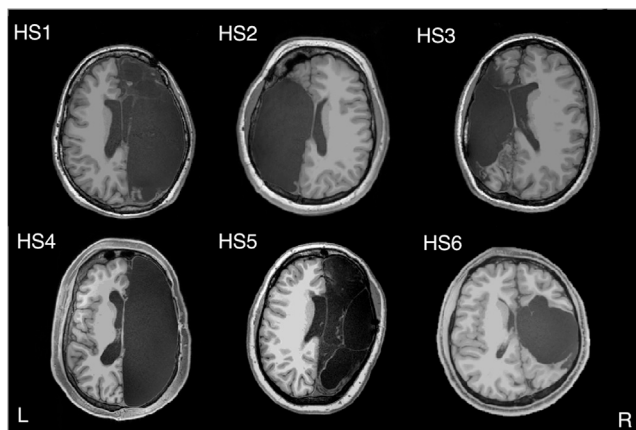
Figure 1. Hemispherectomy Brain Anatomy
Six adult participants with left (n = 2, HS2 and HS3) or right (n = 4, HS1, HS4, HS5, and HS6) hemispherectomy. Axial slices were taken minimally above the anterior/posterior commissure line. L, left; R, right.

patients who had their language-dominant hemisphere resected (Ivanova et al., 2017).

The alterations in brain function that must underlie much of this compensation are poorly understood, and studies of them have almost always been restricted to specific abilities and specific brain regions. Of the few studies investigating brain function in hemispherectomy, most focus exclusively on one modality, such as vision (Bittar et al., 2000; Damásio et al., 1975; Danelli et al., 2013; Georgy et al., 2019; Werth, 2006), somatosensory/ motor function (Bernasconi et al., 2000; Bittar et al., 2000; de Bode and Curtiss, 2000; Graveline et al., 1998; Holloway et al., 2000; Leonhardt et al., 2001; Pilato et al., 2009), audition (Paiement et al., 2008), or language (Danelli et al., 2013; Hertz-Pannier et al., 2002; Ivanova et al., 2017; Liégeois et al., 2008); and only one has more than five patients with fMRI data (Holloway et al., 2000). To the best of our knowledge, no study to date has ever investigated resting-state functional networks across the entire hemisphere in individuals with hemispherectomy.

The current study investigated the organization of resting-state networks in high-functioning adults who had childhood hemispherectomy (HS; n = 6; Figure 1) using high-resolution state-of-the-art neuroimaging methods. We compared intrinsic functional architecture in the intact hemispheres of the HS cases with results from the corresponding single masked hemisphere in two healthy adult control samples. The first control sample (CNT; n = 6) was carefully matched on demographic variables and scanned at the same facility with almost identical sequence parameters. To provide a large-sample dataset that would aid generalizability of our findings, we included a second control sample from a publicly available dataset (Brain Genomics Superstruct Project (GSP); Holmes et al., 2015; n = 1,482). We applied a previously introduced parcellation of seven population-average functional networks (Schaefer et al., 2018; Yeo et al., 2011, 2014, 2015) to the entire hemisphere (400 parcels across the whole brain, with 200 parcels per hemisphere; see Figure 2) in order to study resting-state functional network organization more comprehensively. We used a surface-based registration

approach to achieve the highest sensitivity to individual anatomy (see STAR Methods).

This study addressed three questions building on each other. First, can an atlas-based cortical parcellation scheme based on functional connectivity in healthy individuals also be applied to participants with hemispherectomy? Second, is the functional connectome within each individual reliable across two scanning sessions (fingerprinting; Finn et al., 2015)? Lastly, do the functional networks we find in these participants differ from those found in healthy controls? After confirming the first two questions, we found remarkably typical resting-state networks in participants with HS. The single atypical finding was an abnormally increased functional coupling between different networks (normal within-network connectivity but increased between-network connectivity).

RESULTS

Applying an Atlas-Based, Functional Cortical Parcellation to HS Brains

We required a common parcellation to compare HS brains to controls and began by using a widely accepted (although not unique) cortical parcellation scheme that is based entirely on resting-state correlations (not activations externally induced by sensory stimuli). Briefly, this scheme is based on previously identified networks of functionally coupled regions across the cerebral cortex using a clustering approach, described in detail elsewhere (Yeo et al., 2011, 2015), resulting in seven local networks. Recently, this scheme has been further subdivided into more fine-grained parcellations (Schaefer et al., 2018) related to the seven-network parcellation. Here, we used the 400-parcel parcellation across the whole brain, resulting in 200 parcels per hemisphere. This parcellation size allows for testing parcel- and network-specific homogeneity (i.e., similarity of time series within parcels) as well as connectivity with high specificity while also being in line with the resolution of other commonly used parcellations. We first asked whether this parcellation of the brain into intrinsic functional networks, defined in a large independent sample of healthy subjects (Yeo et al., 2011), could be applied to the HS patients in a meaningful way.

To this end, we tested how similar the intrinsic time-series BOLD response at each parcel's vertex (sampled point on surface) was to (1) the mean response across all vertices in that parcel (within parcel), (2) the mean of parcels inside the same network (inside network), and (3) the mean of outside network parcels (outside network). If the parcellation is applicable in the HS brain, we expected to see the strongest homogeneity of responses within the same parcel, followed by stronger vertex-parcel correlations inside than outside the network. We indeed found this expected pattern of homogeneity across HS and control groups (see Figure 3A and Table S1 for distribution of samples); each HS participant showed higher within-parcel than inside-network homogeneity as well as higher inside- than outside-network homogeneity averaged across networks (see Figure 3B). This confirms that application of a standard atlas-based cortical parcellation after surface-based cortical alignment produces reasonable functionally delineated parcels in patients with HS, enabling us to use this parcellation scheme to make comparisons across subject samples. We note that the

Table 1. Demographic and Neurological Information for HS Participants

Case	HS	Etiol	Onset	Age HS	Sex	Hand	Age	POI	VCI
HS1	R	RS	6 y	7 y	F	R	29	74	105
HS2	L	PNS	3 y	6 y	F	L	22	95	101
HS3	L	PNS	5 y	8 y	F	L	22	89	109
HS4	R	RS	10 y	11 y	M	R	31	86	118
HS5	R	RS	3 y	4 y	F	R	20	95	109
HS6	R	CD	birth	3 m	M	R	21	72	91

CD, cortical dysplasia; HS, hemispherectomy; R, right; L, left; Etiol, etiology; RS, Rasmussen's encephalitis; PNS, perinatal stroke; F, female; M, male; m, month; POI, perceptual organization index; VCI, verbal comprehension index; y, years.

homogeneity results are expected in controls and in particular are not an independent finding in the GSP dataset, since the parcellation was derived from the GSP connectivity data in the first place (Yeo et al., 2011).

Resting-State Networks Are Reliable in HS

We next investigated whether the observed functional connectivity profiles within an individual were reliable across two different measurements (i.e., two runs). We employed a previously introduced method, functional connnectome fingerprinting (Finn et al., 2015). This procedure tests whether two instances of the pattern of functional connectivity acquired from the same individual at different time points (i.e., two scans) are more similar to one another than to the patterns of functional connectivity acquired from other individuals. That is, is the functional connectome sufficiently reliable so that one can re-identify an individual across time?

For the GSP individuals with two runs (n = 1,077), connectome fingerprinting was not successful for n = 98 in the left hemisphere and n = 110 in the right hemisphere. Five out of six individuals in the control group had successful connectome fingerprinting in both hemispheres (see Figure 3C). Five of the six individuals with hemispherectomy also had successful connectome fingerprinting. These findings confirm that functional organization of the brain is discriminative for individuals, even if only one hemisphere of the brain is available and when comparing across a large number of individuals (i.e., n > 1,000). They also suggest normal test-retest reliability of functional connectivity across two runs of ~6–7 min

Figure 2. Parcellation Scheme
Displayed as example on the left inflated hemisphere (fsaverage6 template) are (A, upper row) seven color-coded resting-state-derived connectivity networks (Yeo et al., 2011) (see color to network legend on the right) and (B, lower row) 200 outlined parcels (from the 400 whole-brain parcellation; Schaefer et al., 2018).

within the same scanner session in participants with HS, i.e., their connectomes are relatively stable over time.

Quantifying Within-Network and Between-Network Connectivity in HS

A global criterion for resting-state networks in healthy individuals is overall stronger connectivity of regions within one network and weaker connectivity between regions of different networks. Our primary aim was to quantify this metric also in patients with HS, capitalizing on our unique sample. Given that most resting-state networks are bilaterally distributed across both hemispheres, we expected to find possibly profoundly rearranged networks in the single remaining hemisphere of the HS participants. We thus separately quantified connectivity of parcels belonging to the same network (within-network connectivity) and different networks (between-network connectivity) (see Figure 4A).

The first comparison established representativeness of the six CNT control participants' connectivity to the range of the large-sample GSP controls for within- as well as between-network connectivity. Average strength of functional connectivity in CNT of parcels within and between networks was within the 50th and 66th percentile range of the GSP distribution. Hence, despite differences in magnetic resonance (MR) sequence acquisition and preprocessing, the CNT control participants' connectivity was normally representative as compared to the GSP dataset, justifying further comparisons between control and HS groups.

The comparison of main interest concerned the HS and control samples; within-network connectivity was relatively comparable in distribution (variance: GSP, 0.016; CNT, 0.015; and HS, 0.018) and magnitude across all three samples (Figure 4A; Table S4). This finding was corroborated by seed-based, whole-brain analyses (Figure S1 shows whole-brain results for the example of the precuneus cortex [PCC] parcel seed region, a component of the default mode network). In contrast to similar patterns of within-network connectivity, individuals with hemispherectomy showed notably higher between-network connectivity in comparison to both the CNT and the GSP datasets. In fact, four of the six HS individuals' mean connectivity between parcels across different networks was above the 95th percentile of the GSP distribution, and one was above the 90th percentile (Figures 4A and 4B; Table S5).
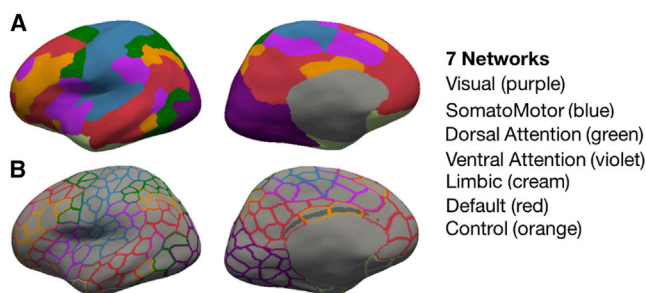
Increased Between-Network Connectivity Is Evident across All Networks in HS Participants

Next, we investigated between-network connectivity of the hemispherectomy participants in more detail. Is the increased
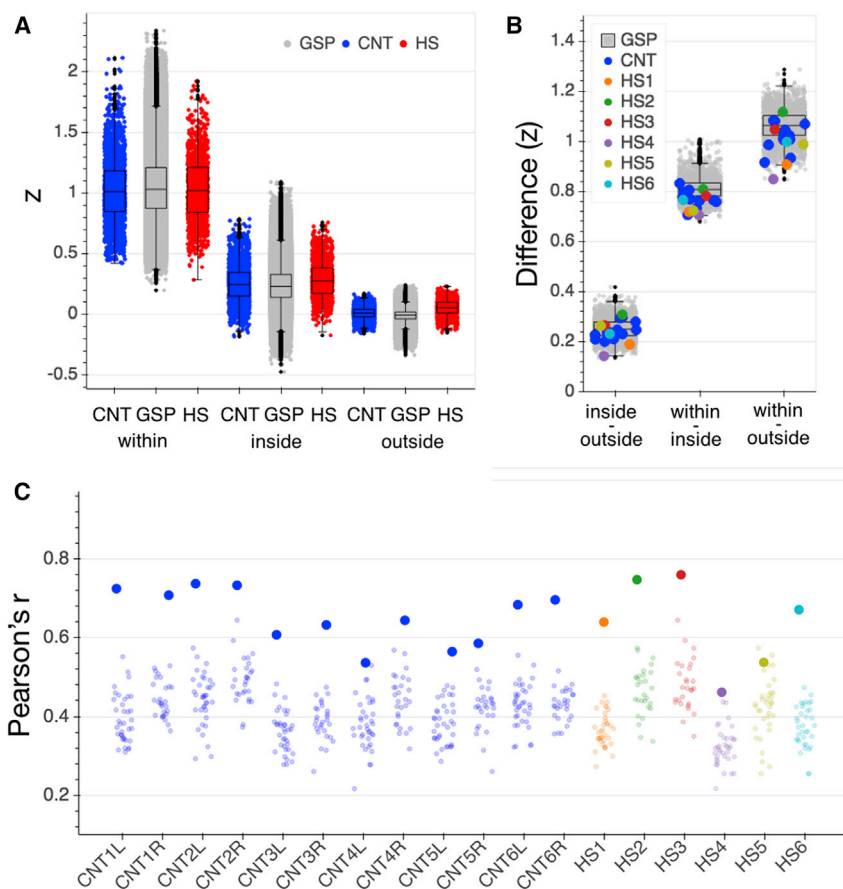
Figure 3. Connectivity Control Analyses

(A) Homogeneity of vertex to parcel time series responses within the originally assigned parcel (within), to all parcels inside the parcel's network (inside), and to all parcels outside the network (outside) for the GSP (gray), CNT (blue) and HS (red) participants. Strengths of correlation (Z) for each comparison in HS were within the normal range of the CNT sample (see Table S1 for statistics). Each data point represents the average correlation for all vertices that comprise a given parcel (200 data points per subject/hemisphere). Boxplots represent distribution of the GSP data.

(B) Differences in strength of correlations between homogeneity comparisons (inside versus outside network, within parcel versus inside network, and within parcel versus outside network) were positive for all HS and control participants. Data points represent individual differences between averaged homogeneity comparisons per hemisphere. Boxplots represent distribution of the GSP data.

(C) Functional connectome fingerprinting per hemisphere. All but one hemisphere in each of the CNT and HS samples (CNT4L and HS5) showed successful connectome fingerprinting; i.e., the functional connectome was most similar across two runs of the same participant (large dots) than in comparison with any other participant (small dots). Boxplots represent distribution of the GSP data. CNT, Caltech control group; GSP, Brain Genomics Superstruct control group; HS, hemispherectomy; L, left hemisphere; R, right hemisphere; Z, Fisher's r to z transformed strength of correlation coefficient.

between-network connectivity mostly driven by some functional networks or evident across all? As illustrated in Figure 4B, stronger between-network connectivity was not specific to only a few networks or a few specific HS participants. Instead, for all seven networks, several hemispherectomy participants exhibited abnormally high connectivity to other networks, outside the normal range, as a detailed quantitative comparison to the control datasets' distributions indicates. Regarding the patients, HS1 and HS6 exhibited the most atypical between-network connectivity; both individuals' strength of correlation per network was higher than that of any control subject (see, Figure 4B and Table S5 for statistics). HS2, HS4, and HS5 also showed connectivity outside the normal range (>90th percentile) for more than at least four of the seven networks. HS3 yielded connectivity between parcels of different networks above the 90th percentile of the GSP sample only for the two sensory networks but remained within the normal range for the others, as well as when comparing to the CNT data. Regarding the networks, the effect was especially pronounced for the somatosensory/motor and visual networks, where all hemispherectomy participants showed remarkably high between-network connectivity (as compared to the GSP sample).

Altered Between-Network Connectivity Patterns Were Idiosyncratic for Some HS Participants

Having established that increased between-network connectivity is found in all hemispherectomy participants (to varying de-

grees) and in all functional networks, we explored the patterns of connectivity in more detail. Previous research has revealed specific relations between certain networks in healthy adults (e.g., anticorrelation between the default mode and the attention networks) (Fox and Raichle, 2007; Fox et al., 2009). Do we find similar patterns of between-network connectivity in hemispherectomy just with an overall increase in the strength of correlation, or does hemispherectomy result in different relations between networks than what is typically reported in healthy adults?

First, we averaged each participant's whole hemisphere connectivity matrix per group (CNT; HS) and plotted resulting sample averages (Figure 5, top row, left and middle panel). In the CNT controls, we replicated previously reported connectivity patterns between networks: the default network parcels were positively temporally correlated with the limbic and control networks, whereas they exhibited little or negative correlations to all other networks. Similarly, the two attention networks were positively correlated with one another, as well as with the somatosensory/motor network. Averaged across all hemispherectomy participants, there were similar patterns of correlation between networks; a stronger positive correlation was found among the default, control, and limbic networks and between most of the attention and sensory networks. However, the observed anticorrelations of the first (default, control, and limbic) and second cluster of networks (attention and sensory) were much less pronounced for HS participants. Overall, it seems that characteristic
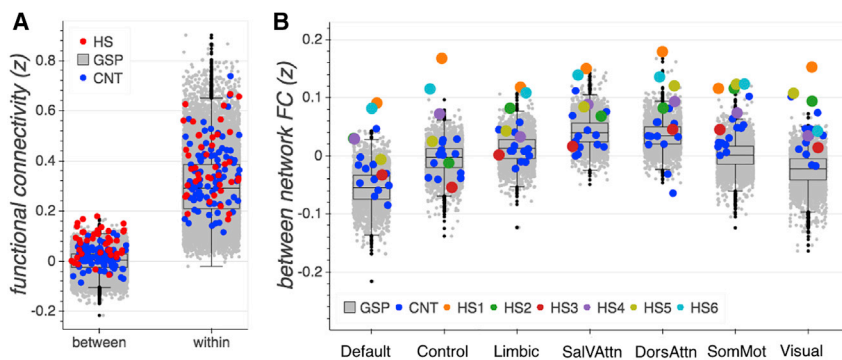
Figure 4. Functional Connectivity

(A) Between- and within-network functional connectivity averaged across networks per group (GSP, CNT, and HS) (seven data points, one for each network, per participant). CNT and HS showed similar within-network connectivity as compared to the large GSP sample, while overall between-network connectivity was notably stronger for HS participants.

(B) High between-network connectivity was evident across all networks and in all but one (HS3) hemispherectomy participant.

Boxplots represent distribution of the GSP data. FC, functional connectivity; Sal/VAttn, salience and ventral attention network; DorsAttn, dorsal attention network; SomMot, somatosensory/motor network; z, Fisher's r to z transformed correlation coefficient. See also Tables S4, S5, and S9.

patterns of between-network connectivity persist after hemispherectomy but with an overall increase.

Second, to investigate potential idiosyncrasy in connectivity for the hemispherectomy participants, we calculated individual connectivity matrices in addition to the averaged sample (Figure 5). HS2, HS3, and HS5 showed patterns generally most similar to those of the control average, with positive correlations within the two network clusters and anticorrelations between these clusters. While HS6 also exhibited similar overall patterns of connectivity to those of controls, there was a notable positive correlation between the somatosensory/motor and all other networks, as well as somewhat more positive correlations between the attention networks and others (mostly with the control and limbic networks). HS1, HS4, and HS6 showed connectivity patterns that were most dissimilar to those observed in controls. HS1 and HS6 showed only positive correlations. Most notably for these three patients, the control network was positively correlated to all others (except the visual network for HS4). Nonetheless, even for those HS subjects with the least typical anticorrelations of functional networks, the clusters of strongest correlations remain generally intact

Third, we explored whether individual differences in connectivity in the HS patients might correspond to increased variance in connectivity across healthy control participants. Variance across all fields of the connectivity matrix in the CNT control sample, however, did not overlap with the most prominent changes in connectivity in hemispherectomy participants (Figure 5, top right), suggesting that the atypical between-network correlations found in our HS patients reflects novel reorganization rather than merely an amplification of normal variability.

In addition to assessing connectivity within and between the specific networks (and their parcels), we also applied tools from graph theory analyses to our data (Sporns, 2014). It should be noted that the interpretation of the network properties in only one hemisphere for the control participants is not a fully valid comparison, because it disregards the influence of homotopic or otherwise cross-hemispheric connections that serve information flow and network distribution in a typical brain with two hemispheres (see Discussion).

We used global efficiency as an estimate of functional integration, i.e., the ability to combine specialized information from distributed brain regions across a hemisphere. Global efficiency is denoted as the average inverse shortest path length in a network (Latora and Marchiori, 2001) and has been related to levels of intellectual functioning, working memory, and attention functioning and overall effective complex cognitive processing (Cohen and D'Esposito, 2016; Kitzbichler et al., 2011; Li et al., 2009; Stanley et al., 2015; van den Heuvel et al., 2017). Four of the six hemispherectomy patients (HS1, HS2, HS5, and HS6) exhibited relatively high global efficiency (above the 95th percentile of the CNT and GSP distribution; see Figure 6A and Table S7) in comparison to the two control groups. Notably, HS1, the participant with the highest between-network connectivity across all networks, surprisingly, did not show the highest global efficiency.

To investigate functional network segregation in one hemisphere, we assessed modularity, defined as the degree to which the overall network may be subdivided into clearly delineated (yet nonoverlapping) groups of nodes (Newman, 2006). Averaging each individual node's modularity values per network revealed rather typical levels for the hemispherectomy participants in comparison to the GSP sample (see Figure 6B and Table S8). Only HS1 (>90th percentile) showed higher modularity in the default mode network.

Relations with In-Scanner Head Motion, Neurological History, and Cognition

To best capture the atypical correlations found in the HS participants, we calculated a summary of between-network connectivity in relation to within-network connectivity as the average strength of between-network connectivity divided by the average strength of within-network connectivity (see STAR Methods).

We first verified that atypical connectivity was not simply the result of high levels of in-scanner head motion. Since head motion affects time series across all networks similarly, this could potentially lead to confounding results suggesting increased connectivity. As outlined in detail in Table S2, two hemispherectomy participants showed elevated levels of head motion. However, it seems unlikely that head motion directly relates to the increased connectivity findings, for two reasons. First, participants that moved the most in the scanner did not show the
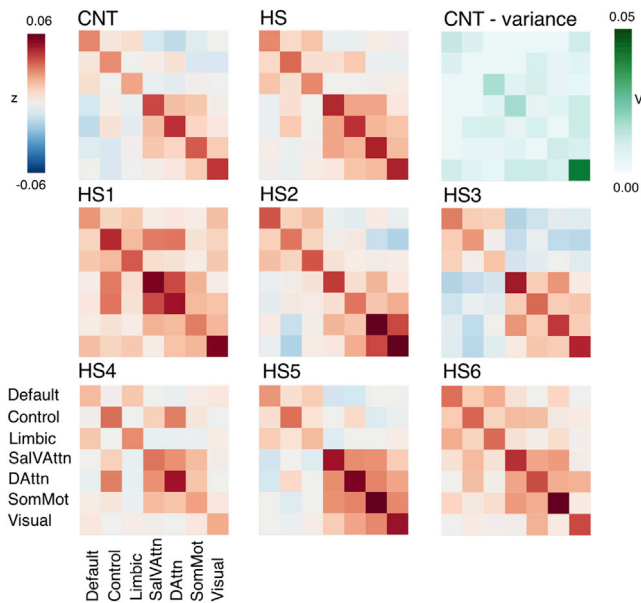
Figure 5. Functional Connectivity Correlation Matrices across Networks

Upper row: averaged connectivity between networks (diagonal = within, off diagonal = between) for the CNT control group (left) showed typical relations between known functional networks (e.g., anticorrelation of default and attention networks). Comparable yet overall stronger connectivity was found across the HS sample (middle). Differences between CNT and HS connectivity did not seem to be pronounced in connections that show greater variance in controls (right). Middle and lower row: connectivity matrix per hemispherectomy participant revealed individual characteristics; between-network connectivity patterns of HS2, HS3, and HS5 were most comparable to controls, while HS4 showed weaker anticorrelations between default and attention networks. HS1 and HS6 showed the strongest connectivity between almost all networks. Sal/VAttn, salience and ventral attention network; DorsAttn, dorsal attention network; SomMot, somatosensory/motor network; V, variance; Z, Fisher's r-to-z transformed strength of correlation. See also Table S6.

highest summary index of connectivity (see Table S6, HS2 and HS4). In fact, participants with the most typical (HS3) and atypical (HS1 and HS6) connectivity between networks showed similar levels of head motion. Second, HS2 and HS4 showed network-specific levels of higher connectivity. If motion would have strongly influenced their connectivity, this would be expected across all networks. These results suggest that the amount of head motion is unlikely to be a confound.

We next explored whether early onset of seizures and subsequently early hemispherectomy was associated with more typical connectivity, but we found no evidence for this (see Table S2). Finally, we explored relationships with cognitive measures, but due to the small sample size, we refrain from presenting any conclusions from this analysis here in the results (see the Supplemental Information and Discussion).

DISCUSSION

The current study provides the first comprehensive analysis of whole-brain functional connectivity across the full repertoire of resting-state networks in a sample of adults with hemispherecto-

my. We used a previously validated functional parcellation of the brain to divide the cortex into 400 parcels (200 in each hemisphere), a fine-grained parcellation that represents seven main functional networks (Yeo et al., 2011) associated with cognitive and sensory functions in humans. We found (1) homogeneous responses across vertices within a parcel, indicating consistency of the chosen parcellation scheme with previous and current parcellations in healthy controls; (2) reliable connectivity patterns across time (scans) in participants (indicated by successful connectome fingerprinting), and (3) overall striking similarity of connectivity patterns that define typical resting-state functional networks in individuals with hemispherectomy. The only atypical finding was that participants with HS, despite having largely typical resting-state networks and connectivity within their nodes, showed abnormally elevated correlations between different networks. Finally, the above findings were not attributable to increased head motion.

Our finding of increased between-network correlations in the HS group is intriguing in light of work on the integration and segregation of brain networks. Changes in characteristics of concerted network connectivity have been reported to correlate with changes in human cognition. For instance, variations in anticorrelation between the default mode and the attention networks have been linked to disrupted brain function and altered states of consciousness, including psychiatric disorders (Buckner et al., 2008), sleep deprivation (De Havas et al., 2012; Yeo et al., 2015), and general anesthesia (Boveroux et al., 2010; Deshpande et al., 2010). At the same time, segregation of nodes and flexible adaptation of functional network organization seem to be integral to adaptive cognitive performance (Hearne et al., 2017). It has been recently suggested that local communication (e.g., within-network connectivity) is essential for motor execution, while integrative communication (e.g., between-network connectivity) is critical for more executive cognitive abilities (e.g., working memory; Cohen and D'Esposito, 2016). Our finding of increased between-network connectivity in HS could thus reflect an adaptive increase in network integration necessary to support overall cognitive functioning and conscious experience despite the loss of typically available brain structure that supports homotopic functional organization. The exact reconfiguration mechanisms in response to task demands (versus the intrinsic organization assessed here with resting state) will be an important next investigation for future studies.

An interesting question is whether the abnormal network metrics reported in this article bear any relation to behavioral symptoms and cognition. While we do not have a large enough sample of patients to investigate this question, we did observe that performance on the Social Responsiveness Scale, full scale IQ, and measures of psychomotor function and executive control were associated with the network-specific increase of between-network connectivity (see Supplemental Information for details). Future work will need to investigate the behavioral correlates of these global network metrics in larger samples. Our preliminiary findings suggest the hypothesis that intact cognitive abilities in individuals with hemispherectomy are accompanied by more typical connectivity, and in turn, that those individuals with the greatest cognitive challenges are the ones who show increased connectivity across functional networks. These initial observations are consistent with the idea that more successful
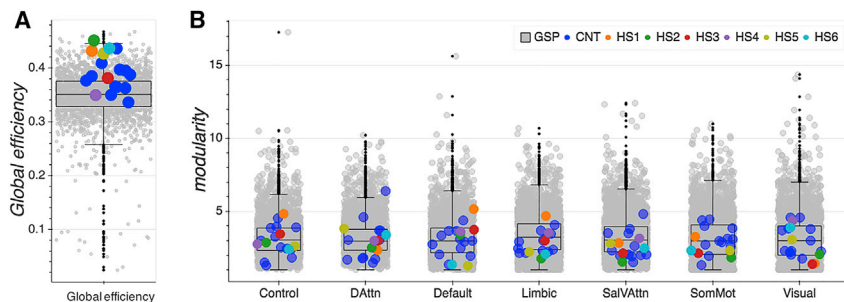
Figure 6. Network Analyses of Functional Integration and Segregation Metrics

Each data point represents data from one participant's hemisphere.

(A) Global efficiency. All hemispherectomy participants showed relative efficient global information processing.

(B) Modularity. Functional segregation of networks was very typical in hemispherectomy participants as compared to both control samples.

Sal/VAttn, salience and ventral attention network; DorsAttn, dorsal attention network; SomMot, somatosensory/motor network. Boxplots represent distribution of the GSP data. See also Tables S7 and S8.

compensation is accompanied by more typical connectivity patterns. Longitudinal studies could further address the complex question of whether these changes are related to compensation and recovery from hemispherectomy.

Our study has several limitations. To address the limitation of small sample size, we presented both group-wise and subject-wise data in the HS patients, and we compared this sample with carefully matched healthy controls, as well as a large normative sample, aiding the interpretability and generalizability of our findings. To address the highly abnormal neuroanatomy (i.e., the loss of one hemisphere) and enable comparisons across groups, we employed a surface-based registration approach that takes individual anatomical features into account more sensitively than possible with a volumetric registration strategy (Fischl et al., 2008; Hinds et al., 2008). We also refrained from registering the functional imaging data directly to a common template and instead applied previously reported anatomical parcellations (Yeo et al., 2011) to each participant's structural brain image and registered their functional data only to their individual anatomy. By doing so, we gained a common reference space (the parcellations in individual anatomy) with high individual anatomical sensitivity to cortical folding pattern.

We chose a rather fine-grained functional parcellation scheme of 200 parcels per individual hemisphere (400 parcels across the whole brain) compared to other often used parcellation schemes (e.g., Gordon et al., 2016). Even finer-grained parcellations (e.g., 500 parcels per hemisphere) might reveal more subtle reorganization; however, they also come at the cost of greater spatial distortions and show increased spatial variability in the typical population (Arslan et al., 2018; Salehi et al., 2018).

One important aspect of the intrinsic functional architecture of the human brain is a homotopic organization of bilaterally distributed functional regions that are strongly interconnected across the left and right hemispheres. Even in complete congenital absence of the corpus callosum, essentially intact homotopic resting-state networks have been reported (Tyszka et al., 2011). One plausible explanation for the largely preserved and bilateral resting-state networks in that population is the presence of other commissural pathways (e.g., the anterior commissure; Tyszka et al., 2011) and possibly the development of alternate interhemispheric connections (Tovar-Moll et al., 2014). It is presumed that the relatively normal levels of cognitive functioning reported in individuals with agenesis of the corpus callosum results from their relatively intact resting-state networks (Paul

et al., 2007; Tyszka et al., 2011). While such white matter abnormalities raise interesting questions about alternate routing of information flow in the brain, (e.g., novel white matter connections; Tovar-Moll et al., 2014), the cortical substrate for typical resting-state networks is still intact in these individuals, presumably supporting bilateral contributions to cognitive abilities.

Our findings raise intriguing new questions about the neural basis of integrated cognition and conscious experience. In our HS patients (with full anatomical resection), there is simply no contralateral hemisphere present at all, eliminating bilateral resting-state networks and the possibility of bilateral contributions to conscious experience.

In sum, the current study provides evidence on the neural reorganization that produces compensated cognition after the surgical removal of one hemisphere. Functional connectivity of the human brain, as measured with resting-state fMRI, leaves open exciting future questions for task-based functional localization in hemispherectomy. Insights from these rare patients argue that intrinsic mechanisms of brain organization in only half of the typically available cortex can be sufficient to support extensive cognitive compensation.

STAR★METHODS

Detailed methods are provided in the online version of this paper and include the following:

- KEY RESOURCES TABLE
- CONTACT FOR REAGENTS AND RESOURCE SHARING
- EXPERIMENTAL MODEL AND SUBJECT DETAILS
  - Caltech dataset
  - Brain Genomics Superstruct Project Dataset
- METHOD DETAILS
  - Brain Genomics Superstruct Project Dataset
  - Caltech Dataset
- QUANTIFICATION AND STATISTICAL ANALYSIS
  - Parcellation
  - Functional connectivity analyses
- DATA AND CODE AVAILABILITY

SUPPLEMENTAL INFORMATION

Supplemental Information can be found online at https://doi.org/10.1016/j.celrep.2019.10.067.

AUTHOR CONTRIBUTIONS

D.K., R.A., J.M.T., and L.K.P. designed the experiments; D.K., J.M.T., L.K.P., and R.N. conducted the experiments; D.K., B.F., and B.T.T.Y. analyzed the data; D.K. and R.A. wrote the paper; and J.M.T., B.F., B.T.T.Y., J.D., and L.K.P. provided feedback for analyses and paper.

DECLARATION OF INTERESTS

B.F. has a financial interest in CorticoMetrics, a company whose medical pursuits focus on brain imaging and measurement technologies. B.F.'s interests were reviewed and are managed by Massachusetts General Hospital and Partners HealthCare in accordance with their conflict of interest policies. All other authors declare no competing interests.

REFERENCES

Andersson, J.L., Skare, S., and Ashburner, J. (2003). How to correct susceptibility distortions in spin-echo echo-planar images: application to diffusion tensor imaging. Neuroimage 20, 870–888.

Arslan, S., Ktena, S.I., Makropoulos, A., Robinson, E.C., Rueckert, D., and Parisot, S. (2018). Human brain mapping: A systematic comparison of parcellation methods for the human cerebral cortex. Neuroimage 170, 5–30.

Bernasconi, A., Bernasconi, N., Lassonde, M., Toussaint, P.J., Meyer, E., Reutens, D.C., Gotman, J., Andermann, F., and Villemure, J.G. (2000). Sensorimotor organization in patients who have undergone hemispherectomy: a study with (15)O-water PET and somatosensory evoked potentials. Neuroreport 11, 3085–3090.

Biswal, B., Yetkin, F.Z., Haughton, V.M., and Hyde, J.S. (1995). Functional connectivity in the motor cortex of resting human brain using echo-planar MRI. Magn. Reson. Med. 34, 537–541.

Bittar, R.G., Ptito, A., and Reutens, D.C. (2000). Somatosensory representation in patients who have undergone hemispherectomy: a functional magnetic resonance imaging study. J. Neurosurg. 92, 45–51.

Boveroux, P., Vanhaudenhuyse, A., Bruno, M.A., Noirhomme, Q., Lauwick, S., Luxen, A., Degueldre, C., Plenevaux, A., Schnakers, C., Phillips, C., et al. (2010). Breakdown of within- and between-network resting state functional magnetic resonance imaging connectivity during propofol-induced loss of consciousness. Anesthesiology 113, 1038–1053.

Buckner, R.L., Andrews-Hanna, J.R., and Schacter, D.L. (2008). The brain's default network: anatomy, function, and relevance to disease. Ann. N Y Acad. Sci. 1124, 1–38.

Castellanos, F.X., Di Martino, A., Craddock, R.C., Mehta, A.D., and Milham, M.P. (2013). Clinical applications of the functional connectome. Neuroimage 80, 527–540.

Cohen, J.R., and D'Esposito, M. (2016). The segregation and integration of distinct brain networks and their relationship to cognition. J. Neurosci. 36, 12083–12094.

Cole, M.W., Bassett, D.S., Power, J.D., Braver, T.S., and Petersen, S.E. (2014). Intrinsic and task-evoked network architectures of the human brain. Neuron 83, 238–251.

Constantino, J.N., and Gruber, C.P. (2012). Social Responsiveness Scale (SRS-2), Second Edition (Torrence, CA: Western Psychological Services).

Cox, R.W. (1996). AFNI: software for analysis and visualization of functional magnetic resonance neuroimages. Comput. Biomed. Res. 29, 162–173.

Damásio, A.R., Lima, A., and Damásio, H. (1975). Nervous function after right hemispherectomy. Neurology 25, 89–93.

Damasio, A.R., Eslinger, P.J., Damasio, H., Van Hoesen, G.W., and Cornell, S. (1985). Multimodal amnesic syndrome following bilateral temporal and basal forebrain damage. Arch. Neurol. 42, 252–259.

Damoiseaux, J.S., Rombouts, S.A., Barkhof, F., Scheltens, P., Stam, C.J., Smith, S.M., and Beckmann, C.F. (2006). Consistent resting-state networks across healthy subjects. Proc. Natl. Acad. Sci. USA 103, 13848–13853.

Danelli, L., Cossu, G., Berlingeri, M., Bottini, G., Sberna, M., and Paulesu, E. (2013). Is a lone right hemisphere enough? Neurolinguistic architecture in a case with a very early left hemispherectomy. Neurocase 19, 209–231.

de Bode, S., and Curtiss, S. (2000). Language after hemispherectomy. Brain Cogn. 43, 135–138.

De Havas, J.A., Parimal, S., Soon, C.S., and Chee, M.W. (2012). Sleep deprivation reduces default mode network connectivity and anti-correlation during rest and task performance. Neuroimage 59, 1745–1751.

Delis, D.C., Kaplan, E., and Kramer, J.H. (2011). Delis-Kaplan Executive Function System®(D-KEFS®): Examiner's Manual: Flexibility of Thinking, Concept Formation, Problem Solving, Planning, Creativity, Impulse Control, Inhibition (Pearson).

Deshpande, G., Kerssens, C., Sebel, P.S., and Hu, X. (2010). Altered local coherence in the default mode network due to sevoflurane anesthesia. Brain Res. 1318, 110–121.

Devlin, A.M., Cross, J.H., Harkness, W., Chong, W.K., Harding, B., Vargha-Khadem, F., and Neville, B.G. (2003). Clinical outcomes of hemispherectomy for epilepsy in childhood and adolescence. Brain 126, 556–566.

Dubois, J., Galdi, P., Paul, L.K., and Adolphs, R. (2018a). A distributed brain network predicts general intelligence from resting-state human neuroimaging data. Philos. Trans. R. Soc. Lond. B Biol. Sci. 373, 20170284.

Dubois, J., Galdi, P., Han, Y., Paul, L.K., and Adolphs, R. (2018b). Resting-state functional brain connectivity best predicts the personality dimension of openness to experience. Personal Neurosci. 1, e6.

Esteban, O., Markiewicz, C.J., Blair, R.W., Moodie, C.A., Isik, A.I., Erramuzpe, A., Kent, J.D., Goncalves, M., DuPre, E., Snyder, M., et al. (2018). fMRIPrep: a robust preprocessing pipeline for functional MRI. Nat. Methods 16, 111–116.

Fan, L., Li, H., Zhuo, J., Zhang, Y., Wang, J., Chen, L., Yang, Z., Chu, C., Xie, S., Laird, A.R., et al. (2016). The Human Brainnetome Atlas: a new brain atlas based on connectional architecture. Cereb. Cortex 26, 3508–3526.

Feuillet, L., Dufour, H., and Pelletier, J. (2007). Brain of a white-collar worker. Lancet 370, 262.

Finn, E.S., Shen, X., Scheinost, D., Rosenberg, M.D., Huang, J., Chun, M.M., Papademetris, X., and Constable, R.T. (2015). Functional connectome finger-printing: identifying individuals using patterns of brain connectivity. Nat. Neurosci. 18, 1664–1671.

Fischl, B., Liu, A., and Dale, A.M. (2001). Automated manifold surgery: constructing geometrically accurate and topologically correct models of the human cerebral cortex. IEEE Trans. Med. Imaging 20, 70–80.

Fischl, B., Salat, D.H., Busa, E., Albert, M., Dieterich, M., Haselgrove, C., van der Kouwe, A., Killiany, R., Kennedy, D., Klaveness, S., et al. (2002). Whole brain segmentation: automated labeling of neuroanatomical structures in the human brain. Neuron 33, 341–355.

Fischl, B., Rajendran, N., Busa, E., Augustinack, J., Hinds, O., Yeo, B.T., Mohlberg, H., Amunts, K., and Zilles, K. (2008). Cortical folding patterns and predicting cytoarchitecture. Cereb. Cortex 18, 1973–1980.

Fox, M.D., and Raichle, M.E. (2007). Spontaneous fluctuations in brain activity observed with functional magnetic resonance imaging. Nat. Rev. Neurosci. 8, 700–711.

Fox, M.D., Zhang, D., Snyder, A.Z., and Raichle, M.E. (2009). The global signal and observed anticorrelated resting state brain networks. J. Neurophysiol. 101, 3270–3283.

Georgy, L., Jans, B., Tamietto, M., and Ptito, A. (2019). Functional reorganization of population receptive fields in a hemispherectomy patient with blindsight. Neuropsychologia 128, 198–203.

Glasser, M.F., Coalson, T.S., Robinson, E.C., Hacker, C.D., Harwell, J., Yacoub, E., Ugurbil, K., Andersson, J., Beckmann, C.F., Jenkinson, M., et al. (2016). A multi-modal parcellation of human cerebral cortex. Nature 536, 171–178.

Gordon, E.M., Laumann, T.O., Adeyemo, B., Huckins, J.F., Kelley, W.M., and Petersen, S.E. (2016). Generation and evaluation of a cortical area parcellation from resting-state correlations. Cereb. Cortex 26, 288–303.

Gorgolewski, K., Burns, C.D., Madison, C., Clark, D., Halchenko, Y.O., Waskom, M.L., and Ghosh, S.S. (2011). Nipype: a flexible, lightweight and extensible neuroimaging data processing framework in python. Front. Neuroinform. 5, 13.

Gorgolewski, K.J., Auer, T., Calhoun, V.D., Craddock, R.C., Das, S., Duff, E.P., Flandin, G., Ghosh, S.S., Glatard, T., Halchenko, Y.O., et al. (2016). The brain imaging data structure, a format for organizing and describing outputs of neuroimaging experiments. Sci. Data 3, 160044.

Graveline, C.J., Mikulis, D.J., Crawley, A.P., and Hwang, P.A. (1998). Regionalized sensorimotor plasticity after hemispherectomy fMRI evaluation. Pediatr. Neurol. 19, 337–342.

Hearne, L.J., Cocchi, L., Zalesky, A., and Mattingley, J.B. (2017). Reconfiguration of brain network architectures between resting-state and complexity-dependent cognitive reasoning. J. Neurosci. 37, 8399–8411.

Hertz-Pannier, L., Chiron, C., Jambaqué, I., Renaux-Kieffer, V., Van de Moortele, P.F., Delalande, O., Fohlen, M., Brunelle, F., and Le Bihan, D. (2002). Late plasticity for language in a child's non-dominant hemisphere: a pre- and post-surgery fMRI study. Brain 125, 361–372.

Hinds, O.P., Rajendran, N., Polimeni, J.R., Augustinack, J.C., Wiggins, G., Wald, L.L., Diana Rosas, H., Potthast, A., Schwartz, E.L., and Fischl, B. (2008). Accurate prediction of V1 location from cortical folds in a surface coordinate system. Neuroimage 39, 1585–1599.

Holloway, V., Gadian, D.G., Vargha-Khadem, F., Porter, D.A., Boyd, S.G., and Connelly, A. (2000). The reorganization of sensorimotor function in children after hemispherectomy. A functional MRI and somatosensory evoked potential study. Brain 123, 2432–2444.

Holmes, A.J., Hollinshead, M.O., O'Keefe, T.M., Petrov, V.I., Fariello, G.R., Wald, L.L., Fischl, B., Rosen, B.R., Mair, R.W., Roffman, J.L., et al. (2015).

Brain Genomics Superstruct Project initial data release with structural, functional, and behavioral measures. Sci. Data 2, 150031.

Ivanova, A., Zaidel, E., Salamon, N., Bookheimer, S., Uddin, L.Q., and de Bode, S. (2017). Intrinsic functional organization of putative language networks in the brain following left cerebral hemispherectomy. Brain Struct. Funct. 222, 3795–3805.

Jenkinson, M. (2003). Fast, automated, N-dimensional phase-unwrapping algorithm. Magn. Reson. Med. 49, 193–197.

Jonas, R., Nguyen, S., Hu, B., Asarnow, R.F., LoPresti, C., Curtiss, S., de Bode, S., Yudovin, S., Shields, W.D., Vinters, H.V., and Mathern, G.W. (2004). Cerebral hemispherectomy: hospital course, seizure, developmental, language, and motor outcomes. Neurology 62, 1712–1721.

Kim, J.S., Park, E.K., Shim, K.W., and Kim, D.S. (2018). Hemispherotomy and functional hemispherectomy: indications and outcomes. J. Epilepsy Res. 8, 1–5.

Kitzbichler, M.G., Henson, R.N., Smith, M.L., Nathan, P.J., and Bullmore, E.T. (2011). Cognitive effort drives workspace configuration of human brain functional networks. J. Neurosci. 31, 8259–8270.

Kong, R., Li, J., Orban, C., Sabuncu, M.R., Liu, H., Schaefer, A., Sun, N., Zuo, X.N., Holmes, A.J., Eickhoff, S.B., and Yeo, B.T.T. (2019). Spatial topography of individual-specific cortical networks predicts human cognition, personality, and emotion. Cereb. Cortex 29, 2533–2551.

Latora, V., and Marchiori, M. (2001). Efficient behavior of small-world networks. Phys. Rev. Lett. 87, 198701.

Leonhardt, G., Bingel, U., Spiekermann, G., Kurthen, M., Müller, S., and Hufnagel, A. (2001). Cortical activation in patients with functional hemispherectomy. J. Neurol. 248, 881–888.

Li, Y., Liu, Y., Li, J., Qin, W., Li, K., Yu, C., and Jiang, T. (2009). Brain anatomical network and intelligence. PLoS Comput. Biol. 5, e1000395.

Liégeois, F., Connelly, A., Baldeweg, T., and Vargha-Khadem, F. (2008). Speaking with a single cerebral hemisphere: fMRI language organization after hemispherectomy in childhood. Brain Lang. 106, 195–203.

Liu, T.T., Nestor, A., Vida, M.D., Pyles, J.A., Patterson, C., Yang, Y., Yang, F.N., Freud, E., and Behrmann, M. (2018). Successful reorganization of category-selective visual cortex following occipito-temporal lobectomy in Childhood. Cell Rep. 24, 1113–1122.e6.

Moosa, A.N., Jehi, L., Marashly, A., Cosmo, G., Lachhwani, D., Wyllie, E., Kotagal, P., Bingaman, W., and Gupta, A. (2013). Long-term functional outcomes and their predictors after hemispherectomy in 115 children. Epilepsia 54, 1771–1779.

Newman, M.E. (2006). Modularity and community structure in networks. Proc. Natl. Acad. Sci. USA 103, 8577–8582.

Paiement, P., Champoux, F., Bacon, B.A., Lassonde, M., Gagné, J.P., Mensour, B., Leroux, J.M., and Lepore, F. (2008). Functional reorganization of the human auditory pathways following hemispherectomy: an fMRI demonstration. Neuropsychologia 46, 2936–2942.

Paul, L.K., Brown, W.S., Adolphs, R., Tyszka, J.M., Richards, L.J., Mukherjee, P., and Sherr, E.H. (2007). Agenesis of the corpus callosum: genetic, developmental and functional aspects of connectivity. Nat. Rev. Neurosci. 8, 287–299.

Pilato, F., Dileone, M., Capone, F., Profice, P., Caulo, M., Battaglia, D., Ranieri, F., Oliviero, A., Florio, L., Graziano, A., et al. (2009). Unaffected motor cortex remodeling after hemispherectomy in an epileptic cerebral palsy patient. A TMS and fMRI study. Epilepsy Res. 85, 243–251.

Power, J.D., Mitra, A., Laumann, T.O., Snyder, A.Z., Schlaggar, B.L., and Petersen, S.E. (2014). Methods to detect, characterize, and remove motion artifact in resting state fMRI. Neuroimage 84, 320–341.

Ramantani, G., Kadish, N.E., Brandt, A., Strobl, K., Stathi, A., Wiegand, G., Schubert-Bast, S., Mayer, H., Wagner, K., Korinthenberg, R., et al. (2013). Seizure control and developmental trajectories after hemispherotomy for refractory epilepsy in childhood and adolescence. Epilepsia 54, 1046–1055.

Rubinov, M., and Sporns, O. (2010). Complex network measures of brain connectivity: uses and interpretations. Neuroimage 52, 1059–1069.

Salehi, M., Karbasi, A., Shen, X., Scheinost, D., and Constable, R.T. (2018). An exemplar-based approach to individualized parcellation reveals the need for sex specific functional networks. Neuroimage *170*, 54–67.

Schaefer, A., Kong, R., Gordon, E.M., Laumann, T.O., Zuo, X.N., Holmes, A.J., Eickhoff, S.B., and Yeo, B.T.T. (2018). Local-global parcellation of the human cerebral cortex from intrinsic functional connectivity MRI. Cereb. Cortex *28*, 3095–3114.

Smith, S.M., Fox, P.T., Miller, K.L., Glahn, D.C., Fox, P.M., Mackay, C.E., Filippini, N., Watkins, K.E., Toro, R., Laird, A.R., and Beckmann, C.F. (2009). Correspondence of the brain's functional architecture during activation and rest. Proc. Natl. Acad. Sci. USA *106*, 13040–13045.

Sporns, O. (2014). Contributions and challenges for network models in cognitive neuroscience. Nat. Neurosci. *17*, 652–660.

Stanley, M.L., Simpson, S.L., Dagenbach, D., Lyday, R.G., Burdette, J.H., and Laurienti, P.J. (2015). Changes in brain network efficiency and working memory performance in aging. PLoS ONE *10*, e0123950.

Tovar-Moll, F., Monteiro, M., Andrade, J., Bramati, I.E., Vianna-Barbosa, R., Marins, T., Rodrigues, E., Dantas, N., Behrens, T.E., de Oliveira-Souza, R., et al. (2014). Structural and functional brain rewiring clarifies preserved interhemispheric transfer in humans born without the corpus callosum. Proc. Natl. Acad. Sci. USA *111*, 7843–7848.

Tustison, N.J., Avants, B.B., Cook, P.A., Zheng, Y., Egan, A., Yushkevich, P.A., and Gee, J.C. (2010). N4ITK: improved N3 bias correction. IEEE Trans. Med. Imaging *29*, 1310–1320.

Tyszka, J.M., Kennedy, D.P., Adolphs, R., and Paul, L.K. (2011). Intact bilateral resting-state networks in the absence of the corpus callosum. J. Neurosci. *31*, 15154–15162.

van den Heuvel, M.P., de Lange, S.C., Zalesky, A., Seguin, C., Yeo, B.T.T., and Schmidt, R. (2017). Proportional thresholding in resting-state fMRI functional connectivity networks and consequences for patient-control connectome studies: Issues and recommendations. Neuroimage *152*, 437–449.

Wechsler, D. (2011). Wechsler Abbreviated Scale of Intelligence, Second Edition (Psychological Corporation).

Werth, R. (2006). Visual functions without the occipital lobe or after cerebral hemispherectomy in infancy. Eur. J. Neurosci. *24*, 2932–2944.

Yeo, B.T., Krienen, F.M., Sepulcre, J., Sabuncu, M.R., Lashkari, D., Hollinshead, M., Roffman, J.L., Smoller, J.W., Zöllei, L., Polimeni, J.R., et al. (2011). The organization of the human cerebral cortex estimated by intrinsic functional connectivity. J. Neurophysiol. *106*, 1125–1165.

Yeo, B.T., Krienen, F.M., Chee, M.W., and Buckner, R.L. (2014). Estimates of segregation and overlap of functional connectivity networks in the human cerebral cortex. Neuroimage *88*, 212–227.

Yeo, B.T., Tandi, J., and Chee, M.W. (2015). Functional connectivity during rested wakefulness predicts vulnerability to sleep deprivation. Neuroimage *111*, 147–158.

STAR★METHODS

KEY RESOURCES TABLE

REAGENT or RESOURCE	SOURCE	IDENTIFIER
Deposited Data		
GSP MRI data	Neuroinformatics Research Group (Harvard University) (NRG) http://www.neuroinfo.org/	https://dataverse.harvard.edu/dataverse/GSP https://doi.org/10.7910/DVN/25833
Caltech MRI and behavioral data	California Institute of Technology, Pasadena, CA, USA	https://openneuro.org/datasets/ds002232
Experimental Models: Organisms/Strains		
Human: patient, controls	Neuroinformatics Research Group (Harvard University) (NRG) http://www.neuroinfo.org/;	N/A
	California Institute of Technology, Pasadena, CA, USA	
Software and Algorithms		
MATLAB, 2017b	Mathworks	https://www.mathworks.com, RRID:SCR_00162
FreeSurfer	Laboratory for Computational Neuroimaging, Athinoula A. Martinos Center for Biomedical Imaging, Charlestown, MA, USA	https://surfer.nmr.mgh.harvard.edu/, RRID:SCR_001847
FSL	Analysis Group, FMRIB, Oxford, UK	https://fsl.fmrib.ox.ac.uk/fsl/fslwiki, RRID:SCR_002823
Functional Brain Parcellation	Computational Brain Imaging Group, National University of Singapore, Singapore	https://github.com/ThomasYeoLab/CBIG/tree/master/stable_projects/brain_parcellation/Schaefer2018_LocalGlobal
Brain Connectivity Toolbox	Rubinov & Sporns (2010)	http://sites.google.com/site/bctnet/, RRID:SCR_004841

CONTACT FOR REAGENTS AND RESOURCE SHARING

Further information and requests for resource should be directed to and will be fulfilled by the lead contact, Dr. Dorit Kliemann, dorit@caltech.edu.

This study did not create new unique reagents.

EXPERIMENTAL MODEL AND SUBJECT DETAILS

Data was either acquired at the California Institute of Technology or obtained from a publicly available dataset of fMRI data, described in detail below.

Caltech dataset

Six adults with hemispherectomy in childhood (HS; 2 males, 2 left-handed, mean age = 24.33 (SD = 4.62) years) and six typically developed adults (CNT; 2 males, 2 left-handed, mean age = 26.8 (SD = 4.26)) were scanned at the Caltech Brain Imaging Center. Participants signed written informed consent prior to participation in accordance with protocols approved by the Institutional Review Board of the California Institute of Technology. These participants were similar with respect to intellectual functioning levels (mean full scale IQ: HS = 90.83 (SD = 7.41), CNT = 95.5 (SD = 3.86)), age, handedness, and sex. Demographic sample information as well as detailed previous and current neurological history about the individuals with HS is provided in the Supporting Information (Table S3). In an exploratory analysis (see Table S9), we further assessed intellectual and cognitive abilities in relation to functional connectivity with the following measures: intellectual functioning (WAIS-III, (Wechsler, 2011), executive function (D-KEFS, Delis-Kaplan Executive Function System (Delis et al., 2011); social function (Social Responsiveness Scale-2 Adult Self report (Constantino and Gruber, 2012), SRS-2).

Hemispherectomy cases

The dataset included four individuals with right and two with left hemispherectomy with different etiology (L-HS, perinatal stroke n = 2; R-HS: Rasmussen encephalitis n = 3, cortical dysplasia n = 1), age at seizure onset (minutes after birth to 10 years-old) and age at hemispherectomy surgery (3 month – 11 years-old; see Supplemental Information, Table S1).

Four individuals underwent functional hemispherectomy, i.e., large sections of the affected hemisphere were resected and all connections of remaining tissue to the functional hemisphere were disconnected. Two patients had a complete anatomical hemispherectomy. Presence of any missed connections (i.e., complete disconnection of remaining tissue) was assessed by two neurosurgeons specialized in hemispherectomy surgeries (A.F., H.W.P).

Brain Genomics Superstruct Project Dataset
We compared both HS and CNT data to publicly available data from the Brain Genomics Superstruct Project (GSP, https://www.neuroinfo.org/gsp/), collected from 1482 healthy young adults (621 males, mean age = 21.53 years) at Harvard University and the Massachusetts General Hospital (Holmes et al., 2015). Raw data was processed by the laboratory of B.T.T.Y. at Singapore University within the context of previous publications (Schaefer et al., 2018, Kong et al., 2019)

METHOD DETAILS

Brain Genomics Superstruct Project Dataset
Data from GSP were acquired on matched 3 Tesla TIM Trio scanners (Siemens Healthcare, Erlangen, Germany) at the Massachusetts General Hospital and Harvard University with the vendor-supplied 12-channel phased-array head coil. Details on the data collection are described elsewhere (Holmes et al., 2015; Yeo et al., 2011). In short, each subject had one (n = 405) or two (n = 1077) T2*-weighted EPI resting state runs (3 mm isotropic voxel size, TR = 3.0 s, duration 6 min 12 s) and one structural MR scan (1.2 mm isotropic voxel size).

Preprocessing is described in detail elsewhere (Holmes et al., 2015; Kong et al., 2019). In short, processing steps included slice-time correction, motion correction, motion time-point outlier detection (frame wise displacement (FD) > 0.2 mm, voxel-wise differentiated signal variance (DVARS) > 50, uncensored segments of data lasting less than 5 contiguous volumes by FD/DVARS (Gordon et al., 2016)), regression of nuisance variables (global signal (GSR), six motion correction parameters, ventricular signal, white-matter signal, and their temporal derivatives), interpolation (Power et al., 2014) across motion outlier time-points and application of band-pass filtering (0.009 Hz $\leq$ f $\leq$ 0.08 Hz). Preprocessed functional data was subsequently projected onto FreeSurfer fsaverage6 surface space (1mm vertex spacing), smoothed using a 6 mm full-width half-maximum (FWHM) kernel, and downsampled to the fsaverage5 surface space (4 mm vertex spacing) for functional connectivity analyses.

Caltech Dataset
Data from six individuals with hemispherectomy and six control participants were acquired at the Caltech Brain Imaging Center (CBIC) using a 3 Tesla MRI scanner (five CNT and five HS: Magnetom TIM Trio; one CNT and one HS: Magnetom Prisma, Siemens Medical Solutions, Erlangen, Germany) with almost identical imaging parameters. For each participant, we analyzed T1w structural data (MP-RAGE, TR/TE/TI = 1590ms/2.7ms/800ms, 1 mm (TIM Trio) or 0.9mm (Prisma) isotropic voxel size, flip angle = 10°) and two runs of T2*-weighted EPI (TR = 1000ms and 400 images, 6 minutes and 40 s (TIM Trio) or 700ms and 600 images, 7 minutes (Prisma), TE = 30ms, flip angle = 60° (TIM Trio) or 53° (Prisma), 2D multiband acquisition (Multiband acceleration factor = 6) with 2.5 mm isotropic voxels). For the participants acquired with the TIM TRIO, gradient echo field mapping data was acquired with identical geometry to the EPI data for EPI off-resonance distortion correction (TR/TE = 400/5 ms, flip angle = 45°), for the Prisma, two SE-EP images with opposite phase encode directions (TR/TE = 5005/48 ms, flip angle = 90°).

Raw DICOM images were converted to Nifti-1 format files and organized according to the BIDS convention (Gorgolewski et al., 2016; https://bids.neuroimaging.io/) with the docker version of BIDSKIT version 1.0.0 (https://github.com/jmtyszka/bidskit). After conversion, minimal preprocessing was performed using FMRIPREP version 1.0.7, a Nipype based tool (Esteban et al., 2018; Gorgolewski et al., 2011). Each T1-weighted (T1w) volume was corrected for intensity non-uniformity using N4BiasFieldCorrection v2.1.0 (Tustison et al., 2010) and skull-stripped using antsBrainExtraction.sh v2.1.0 (using the OASIS template). Segmentation of cerebrospinal fluid, white matter and gray matter was performed on the brain-extracted T1w using FAST (FSL v5.0.9). Functional EPI data was motion corrected using MCFLIRT (FSL v5.0.9). Susceptibility distortion correction was performed using an implementation of the TOPUP technique (Andersson et al., 2003) using 3dQwarp v16.2.07 distributed as part of AFNI (Cox, 1996) for the two participants with SE-EPI images and with FUGUE v5.0.9 (Jenkinson, 2003) tool for all other participants with GRE fieldmaps. This was followed by spatial co-registration to the individual's T1w control image using boundary-based registration with 9 degrees of freedom, using FLIRT (FSL). FD and DVARS metrics were calculated for each functional run using the methods implemented by Nipype.

Preprocessing of the structural and functional data was conceptually very similar to the above-described GSP data processing with some differences: structural processing with FreeSurfer was performed with version 6.0 for control subjects and developmental version of FreeSurfer (Fischl et al., 2001; Fischl et al., 2002) for the hemispherectomy subjects to allow for reconstruction of acallosal surface space in only one hemisphere. For all participants, data was carefully inspected and manual corrections applied where necessary. The level of necessary manual intervention for HS and CNT data was comparable and the quality of the surface estimation was typical. For the HS participants, only the functional hemisphere was analyzed and subsequently segmented. Interpolation over motion-censored time-points was performed with linear interpolation (versus least estimated squares). Band-pass filtering was

performed with a Butterworth filter (0.009 Hz $\leq$ f $\leq$ 0.08 Hz). Given the significantly shorter TR, no slice timing correction was applied. Functional data was projected onto each subjects' native anatomical space only once, to reduce distortion of multiple surface projections of the atypical hemispherectomy anatomy.

Psychiatric and neurological patient populations often exhibit greater levels of in-scanner head motion. As expected, we also found minimally elevated levels of head motion in some HS participants (see Supplementary Information, Table S2). To counteract data loss due to extensive motion time-point censoring, we applied a slightly more lenient FD threshold (0.4 mm). We discuss motion in detail below. It is unlikely that the aforementioned minimal differences in preprocessing would lead to notable differences in the final connectivity estimation and comparisons between the samples. The main purpose of the GSP data is to provide a reference frame for *both* control and HS individuals, not to make specific claims about differences to the Caltech sample.

QUANTIFICATION AND STATISTICAL ANALYSIS

Parcellation
We used a parcellation into 7 larger, previously described, functional resting state networks and their respective sub-parcellations, into 400 bilateral parcels with 200 parcels per hemisphere (Schaefer et al., 2018, Yeo et al., 2011, 2015).

Functional connectivity analyses
Preprocessed timeseries data was extracted from the surface for cortical regions and averaged within each parcel. To investigate functional connectivity between brain regions, each parcel's timeseries data was correlated with all other parcels per run (excluding outlier time points) using Pearson correlation. For statistical comparisons, the resulting correlation coefficients were then Fisher r-to-z-transformed, resulting in a N_s (number of subjects) x N_r (number of runs) x N_p (number of parcels) connectivity matrix. All analyses were done separately for a hemisphere for control participants, similar to single hemisphere data in hemispherectomy participants.

Parcel homogeneity
To investigate homogeneity (and consistency) of functional connectivity within-parcel at the level of individual subjects we investigated how well each vertex's timeseries represented the average timeseries of its containing parcel. For each subject and run, we first calculated the Pearson correlation, r, between a vertex's timeseries and the average timeseries of i) the assigned parcel without the tested vertex (within-parcel), ii) other parcels belonging to the same network of the vertex's containing parcel (inside-network) and iii) all parcels outside of the network (outside-network). Individual correlations were Fisher z transformed before averaging across conditions. We performed GSP homogeneity analyses on the fsaverage6 surface space, since it is the source space for the creation of the 400 Schaefer parcels. Note that we do not make new inferences about the parcellation's homogeneity or validity based on the GSP analyses, instead these results are only for creating a normative comparison for the HS and CNT samples. One GSP subject's data was excluded from homogeneity analyses due to a registration problem.

Connectome Fingerprinting
To assess reliability of functional connectivity within an individual across different measurements we conducted an analysis known as connectome fingerprinting (described in detail elsewhere (Finn et al., 2015)). In short, we correlated each participant's connectivity matrix i) across the two runs of the same subject and ii) with all runs of all other subjects. If the highest correlation was found between the two runs of the same subject, connectome fingerprinting was deemed "successful" suggestive of reliable patterns of functional connectivity across two runs within an individual. Since some GSP participants only had one run of resting-state fMRI available, comparisons for the left hemisphere included 1087 participants (HS n = 4, CNT n = 6, GSP n = 1077) and for the right hemisphere 1085 participants (HS n = 2, CNT n = 6, GSP n = 1077).

Functional network connectivity
To probe global network characteristics, we tested within-network and between-network connectivity by comparing connectivity between parcels of the same network and parcels of different networks, respectively. To establish the strength of within-network connectivity we averaged Fisher z-transformed correlation values between all parcels of each of the 7 networks. Similarly, the strength of between-network connectivity was calculated by averaging the strength of edges between parcels of each of the 7 networks and all others. This resulted in 7 within- and 7 between-network summary connectivity strengths per participant. We created a summary index (see Table S6) ($Index_{FC}$) of between-network in relation to within-network connectivity as the quotient of between-network connectivity (FC_{Btw}) and within-network connectivity (FC_{Wthn}), for each of the 7 networks:

$$Index_{FC} = FC_{Btw}/FC_{Wthn}$$

Graph theoretical analyses
Graph theoretical analyses have become an important tool to investigate topological aspects of functional brain connectivity (and dysconnectivity) across different patient populations. We calculated the global efficiency and modularity metrics based on thresholded ($z > 0.5$) and binarized individual connectivity matrices (200x200). To explore potentially new functional segregation of network nodes we chose not to use a proportional thresholding approach (see, van den Heuvel et al., 2017, for further discussion). Graph metrics were calculated with a publicly available MATLAB toolbox (Rubinov and Sporns, 2010; brain-connectivity-toolbox.net) for each participant's hemisphere separately (note that this approach results in two data points per control participant).

Classic statistical null hypothesis testing is not statistically meaningful for small patient population samples. We provide quantitative comparisons for the conclusions drawn in this study by a quantitative description of where in the normative distribution of the control sample each individual hemispherectomy participant's relevant connectivity metric falls. This information is reported in the respective results section.

DATA AND CODE AVAILABILITY

The GSP dataset is available at https://dataverse.harvard.edu/dataverse/GSP (https://doi.org/10.7910/DVN/25833). The Caltech control data is available from (https://openneuro.org/datasets/ds002232). The hemispherectomy data is currently only available upon request due to pending IRB decisions. If the data will be made publicly available in the future, it will be deposited into the Caltech control repository. Code to preprocess and create FC for the GSP data is available at https://github.com/ThomasYeoLab/CBIG, subsequent GSP analyses and code to process Caltech datasets is available from the corresponding author upon request (https://github.com/doritdorit/).

Supplemental Information

Intrinsic Functional Connectivity of the Brain

in Adults with a Single Cerebral Hemisphere

Dorit Kliemann, Ralph Adolphs, J. Michael Tyszka, Bruce Fischl, B.T. Thomas Yeo, Remya Nair, Julien Dubois, and Lynn K. Paul
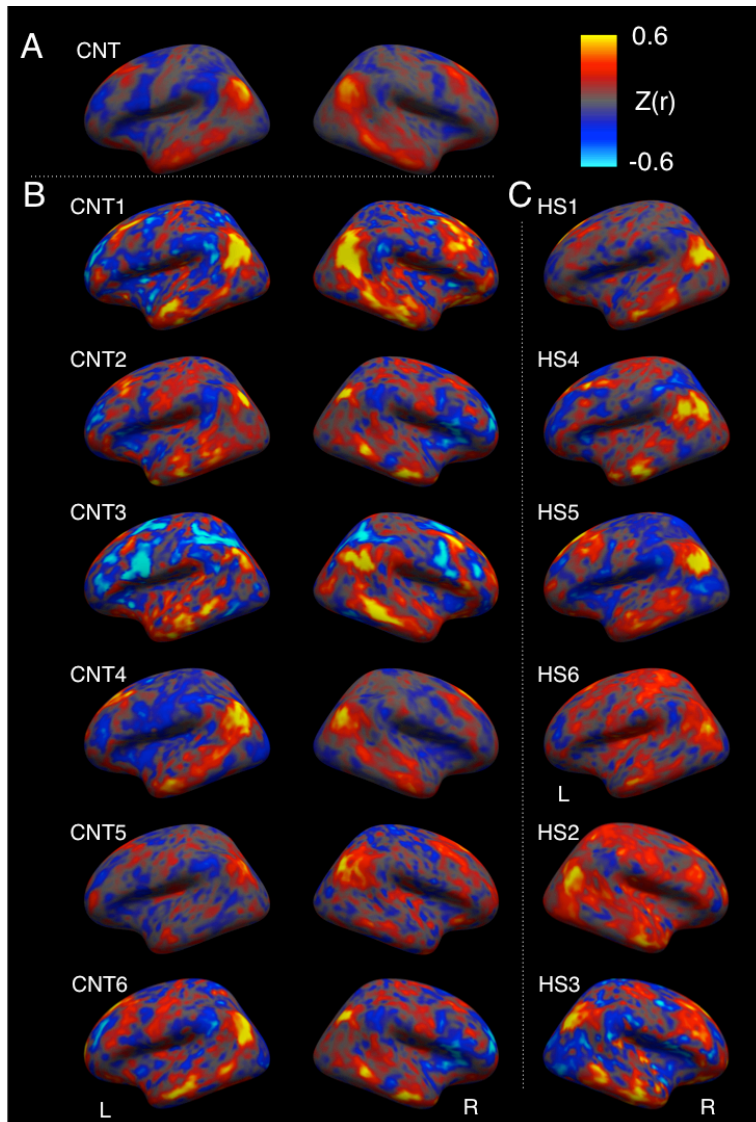
Figure S1. Seed region analysis of the default mode network displayed across the surface per hemisphere, related to **Figure 4A**. Connectivity of the precuneus cortex parcel (PCC) seed region per hemisphere averaged across CNT participants (A), and for each CNT (B) and HS (C) participant. *Abbreviations*: CNT, Caltech Control participant; HS1-6, Hemispherectomy participant; L, left; R, right; Z(r), Fisher's r to z transformed correlation coefficient.

To visualize HS and CNT subjects' data in a common surface space, we performed additional analyses with similar preprocessing as the main analyses except that we registered individual functional data first to the fsaverage6 template, smoothed the data (FWHM = 6mm) and then downsampled the resulting timeseries data onto the fsaverage5 template (following preprocessing procedures described elsewhere (Kong et al., 2018, Schaefer et al., 2018)). Then for each hemisphere, we performed an exemplary seed region analysis across the whole hemisphere, using the PCC parcel of the default mode network parcellation (Yeo et al., 2011) as seed region.

group	cond	mean	std	min	25%	50%	75%	90%	95%	max
	within	1.025	0.257	0.422	0.846	1.012	1.185	1.359	1.475	2.114
CNT	inside	0.252	0.144	-0.182	0.152	0.247	0.345	0.432	0.493	0.786
	outside	0.009	0.050	-0.156	-0.021	0.011	0.043	0.070	0.086	0.171
	within	1.051	0.249	0.198	0.873	1.031	1.210	1.385	1.493	2.339
GSP	inside	0.241	0.142	-0.472	0.142	0.231	0.330	0.428	0.491	1.091
	outside	-0.011	0.048	-0.334	-0.037	-0.006	0.019	0.043	0.059	0.240
	within	1.037	0.268	0.284	0.840	1.020	1.213	1.394	1.499	1.923
HS	inside	0.287	0.156	-0.171	0.172	0.275	0.383	0.502	0.573	0.757
	outside	0.053	0.064	-0.148	0.011	0.054	0.099	0.134	0.156	0.230

Table S1. Homogeneity, related to **Figure 3**. Within-parcel (within), inside-network (inside) and outside-network (outside) vertex-to-parcel timeseries correlation (Fisher r-to-z transformed strength of correlation) averaged across all networks per group (HS, GSP, CNT). *Abbreviations:* CNT, Caltech controls; GSP, Brain Genomic Superstruct controls; HS, hemispherectomy; cond, condition; min, minimum; max, maximum; std, standard deviation from the mean.

ID	FD	DVARS	POI	VCI	Age	Sex	Handedness
HS1	0.10	20.58	74	105	29	F	R
HS2	0.22	27.09	95	101	22	F	L
HS3	0.10	24.75	89	109	22	F	L
HS4	0.21	27.42	86	118	31	M	R
HS5	0.16	25.97	95	109	20	F	R
HS6	0.11	25.33	72	91	21	M	R
CNT1	0.08	22.56	94	106	28	F	L
CNT2	0.16	27.82	104	94	27	F	L
CNT3	0.10	26.82	87	95	34	F	R
CNT4	0.15	31.80	98	90	21	M	R
CNT5	0.09	28.13	92	100	26	M	R
CNT6	0.07	22.80	95	98	25	F	R

Table S2. Demographics, motion and intellectual functioning matching information for CNT and HS group, related to **Table 1**. *Abbreviations*: CNT, Caltech Controls; DVARS, variations in temporal derivatives of timecourse; F, female; FD, mean framewise displacement; FSIQ, full scale IQ; HS, hemispherectomy; ID, participant specific identification; L, left; M, male; POI, perceptual organization index; R, right; VCI, verbal comprehension index.

ID	HS-age (months)	onset (months)	FSIQ	SRS-2	D-KEFS Trails	D-KEFS Tower
HS1	96	72	84	61	1	6
HS2	75	36	95	64	10	10
HS3	96	60	91	56	2	10
HS4	142	130	99	54	4	7
HS5	48	60	96	56	12	9
HS6	3	0	80	45	13	13

Table S3. Neurological history and cognitive function information for hemispherectomy participants, related to **Table 1**. *Abbreviations*: D-KEFS, Delis-Kaplan Executive Function System; FSIQ, Full scale IQ as estimated by WAIS-III; HS, hemispherectomy; ID, participant specific identification; onset, age at epilepsy onset; SRS-2, Social Responsiveness Scale-2 Adult Form Self-Report; D-KEFS Tower: Tower Test of the D-KEFS; D-KEFS Trails: Trail Making Test of the D-KEFS.

	GSP	CNT	HS1	HS2	HS3	HS4	HS5	HS6
mean	0.30	0.35	0.43	0.45	0.35	0.30	0.43	0.41
std	0.13	0.12	0.12	0.15	0.12	0.11	0.17	0.10
min	-0.02	0.12	0.26	0.32	0.17	0.19	0.19	0.33
50%	0.29	0.34	0.45	0.38	0.34	0.28	0.50	0.39
75%	0.39	0.42	0.53	0.54	0.44	0.33	0.54	0.42
90%	0.47	0.50	0.56	0.66	0.47	0.40	0.59	0.51
95%	0.52	0.55	0.56	0.66	0.48	0.45	0.61	0.57
max	0.90	0.74	0.57	0.67	0.49	0.51	0.63	0.62

Table S4. Within-network connectivity values per control groups and hemispherectomy participants averaged across networks, related to **Figure 4A.** None of the hemispherectomy participants' mean values were above the 90th percentile of the control groups. *Abbreviations*. CNT, Caltech controls; GSP, Brain Genomic Superstruct controls; HS, hemispherectomy; max, maximum; min, minimum; std, standard deviation of the mean.

		Default	Control	Limbic	Sal/VAttn	DorsAttn	SomMot	Visual	All
GSP	*mean*	-0.05	4.7 e-3	0.01	0.04	0.04	1.2 e-3	-0.02	7.9 e-4
	std	0.03	0.03	0.02	0.02	0.02	0.03	0.03	0.04
	0.75	-0.03	0.01	0.03	0.06	0.05	0.02	0.00	0.03
	0.90	-0.02	0.03	0.04	0.07	0.06	0.03	0.01	0.05
	0.95	4.0 e-3	0.03	0.05	0.08	0.07	0.04	0.02	0.06
	0.99	0.04	0.10	0.11	0.15	0.17	0.12	0.07	0.18
CNT	*mean*	-0.03	-0.01	0.01	0.04	0.03	0.04	0.03	0.35
	std	0.03	0.03	0.02	0.03	0.04	0.03	0.03	0.02
	0.75	-0.02	0.01	0.02	0.05	0.06	0.05	0.05	0.04
	0.90	3.6 e-3	0.03	0.04	0.08	0.06	0.06	0.07	0.05
	0.95	0.02	0.03	0.05	0.09	0.07	0.08	0.09	0.06
	max	0.05	0.03	0.06	0.11	0.08	0.10	0.10	1.7
HS1	*mean*	0.09	0.17	0.12	0.15	0.18	0.12	0.15	0.14
HS2	*mean*	0.03	-0.01	0.08	0.07	0.08	0.12	0.09	0.07
HS3	*mean*	-0.03	-0.05	0.00	0.02	0.05	0.05	0.01	5.0 e-3
HS4	*mean*	0.03	0.07	0.03	0.09	0.09	0.07	0.03	0.06
HS5	*mean*	-0.01	0.02	0.04	0.08	0.12	0.12	0.11	0.07
HS6	*mean*	0.08	0.12	0.11	0.14	0.14	0.12	0.04	0.11

Table S5. Between-network connectivity values per control groups and hemispherectomy participants as a function of networks and averaged across networks (All), related to **Figure 4B**. *Abbreviations.* CNT, Caltech controls; DorsAttn, dorsal attention network; GSP, Brain Genomic Superstruct controls; HS, hemispherectomy**;** max, maximum; Sal/VAttn, salience and ventral attention network; SomMot, somatosensory/motor network; std, standard deviation of the mean.

ID	Summary index	Default index	Control index	Limbic index	Sal/VAttn index	DorsAttn index	SomMot index	Visual index
HS1	0.33	0.35	0.37	0.32	0.27	0.36	0.38	0.27
HS2	0.14	0.08	-0.04	0.22	0.16	0.26	0.18	0.14
HS3	0.00	-0.11	-0.21	0.01	0.03	0.13	0.11	0.03
HS4	0.20	0.15	0.22	0.12	0.27	0.19	0.31	0.16
HS5	0.15	-0.02	0.08	0.23	0.17	0.21	0.20	0.21
HS6	0.27	0.25	0.33	0.32	0.31	0.35	0.20	0.11

Table S6. Summary index (strength of average between-network connectivity divided by strength of average within-network connectivity) averaged across all networks and per network for hemispherectomy participants, related to **Figures 5 and 6**. *Abbreviations.* DorsAttn, dorsal attention network; HS, hemispherectomy**;** Sal/VAttn, salience and ventral attention network; SomMot, somatosensory/motor network.

group/ID	value	GE
GSP	mean	0.349
	std	0.043
	min	0.024
	50%	0.351
	75%	0.375
	90%	0.395
	95%	0.407
	max	0.467
CNT	mean	0.380
	std	0.027
	min	0.336
	50%	0.381
	75%	0.395
	90%	0.408
	95%	0.421
	max	0.436
HS1	mean	0.432
HS2	mean	0.451
HS3	mean	0.381
HS4	mean	0.349
HS5	mean	0.427
HS6	mean	0.437

Table S7. Global efficiency per control groups and hemispherectomy participants, related to **Figure 6A.**
Abbreviations. CNT, Caltech controls; GSP, Brain Genomic Superstruct controls; HS, hemispherectomy**;** max, maximum; min, minimum; std, standard deviation of the mean.

		Default	Control	Limbic	SalVAttn	DorsAttn	SomMot	Visual
GSP	*mean*	3.245	3.219	3.171	3.384	3.268	3.213	3.258
	std	1.317	1.270	1.403	1.411	1.443	1.557	1.651
	min	1.000	1.000	1.000	1.000	1.000	1.000	1.000
	50%	3.045	2.957	2.974	3.231	3.040	2.974	3.000
	75%	3.864	3.783	3.865	4.154	3.955	4.075	4.000
	90%	4.800	4.870	4.885	5.154	5.160	5.250	5.290
	95%	5.667	5.733	5.692	5.923	6.045	6.027	6.323
	max	17.267	10.217	15.615	10.692	12.409	11.000	14.367
CNT	*mean*	2.891	2.880	2.827	2.672	2.957	3.117	3.029
	std	0.845	1.049	0.652	1.003	1.470	0.946	1.021
	min	1.359	1.300	2.154	1.520	1.478	1.324	1.767
	50%	2.952	2.767	2.692	2.183	2.761	3.038	2.650
	75%	3.428	3.877	3.173	3.505	3.696	3.888	3.808
	90%	3.673	3.950	3.669	3.772	4.517	4.360	4.506
	95%	3.993	4.215	3.865	4.258	5.411	4.427	4.581
	max	4.385	4.533	4.077	4.818	6.391	4.460	4.581
HS1	*mean*	5.1538	4.833	4.692	2.840	2.348	3.275	1.433
HS2	*mean*	3.4231	2.864	1.769	1.546	2.522	1.838	2.065
HS3	*mean*	3.75	3.455	3.000	2.136	3.000	2.135	1.387
HS4	*mean*	3.6154	2.767	3.539	3.160	3.000	2.325	4.367
HS5	*mean*	1.2821	2.633	2.231	2.800	3.826	2.325	3.067
HS6	*mean*	1.359	2.400	2.077	2.480	3.391	2.325	3.900

Table S8. Modularity per network and control sample and hemispherectomy participant, related to **Figure 6B.** *Abbreviations*. CNT, Caltech controls; DorsAttn, dorsal attention network; GSP, Brain Genomic Superstruct controls; HS, hemispherectomy**;** Sal/VAttn, salience and ventral attention network; SomMot, somatosensory/motor network; max, maximum; min, minimum; std, standard deviation of the mean.

	SRS-2	FSIQ	D-KEFS Tower	D-KEFS Trails
Default Mode	$r_s(5) = -0.12$	-	-	-
Limbic	$r_s(5) = -0.17$	-	-	-
Sal/VAttn	-	$r_s(5) = -0.2$	-	-
DorsAttn	-	$r_s(5) = -0.6$	-	-
Control	-	-	$r_s(5) = -0.41$	$r_s(5) = -0.02$
SomMot	-	-	$r_s(5) = -0.64$	-

Table S9 related to **Figure 4B.** Exploratory analyses of brain-behavior relationships between network-specific connectivity (summary index) and cognitive abilities. We a priori decided to explore only those associations for

which there are entries in the table. The SRS-2, a measure of social cognition, showed only very weak to weak negative correlations with increased between-network connectivity (relative to within-network connectivity) within the default mode as well as the limbic networks. Full-scale IQ was only weakly negatively correlated with network-specific connectivity in the ventral attention network, but showed a strong negative correlation with connectivity in the dorsal attention network. For executive control, there was a moderate negative correlation between connectivity in the control network with the D-KEFS Tower Test (measuring spatial planning, rule learning, inhibition and ability to maintain and establish instructional set). The D-KEFS Trail Making Test (a visual-motor sequencing task that indexes flexibility of thinking) revealed no substantial correlation with connectivity of the control network. Since the Tower Test also involves the motor system (psychomotor processing speed), we additionally investigated its possible correlation with connectivity in the somatosensory/motor network and found indeed a strong negative association. These exploratory analyses will require future *a priori* tests in additional samples to establish their reliability. Nonetheless, it is striking that all correlations we found were of negative direction. While exploratory and preliminary, this overall pattern of results might suggest that greater between-network connectivity is associated with more impaired cognitive abilities. This needs to be validated in future studies and larger populations. Given the small sample size we refrain from reporting any p-values since no inference of statistical significance is justified.

Abbreviations. D-KEFS, Delis-Kaplan Executive Function System; DorsAttn, dorsal attention network; FSIQ, Full scale IQ as estimated by WAIS-III; HS, hemispherectomy; ID, participant specific identification; onset, age at epilepsy onset; r_s, Spearman's rank correlation; Sal/VAttn, salience and ventral attention network; SomMot, somatosensory/motor network; SRS-2, Social Responsiveness Scale-2 Adult Form Self-Report; D-KEFS Tower: Tower Test of the D-KEFS; D-KEFS Trails: Trail Making Test of the D-KEFS.